Guided Assembly of Tetramolecular G-Quadruplexes

Liliya A. Yatsunyk,[†,‡,§,*] Olivier Piétrement,[⊥] Delphine Albrecht,[†,‡] Phong Lan Thao Tran,[†,‡,△] Daniel Renčiuk,[†,‡] Hiroshi Sugiyama,[∥] Jean-Michel Arbona,[#] Jean-Pierre Aimé,[#] and Jean-Louis Mergny[†,‡,*]

[†]ARNA Laboratory, University of Bordeaux, F-33000 Bordeaux, France, [‡]INSERM U869, IECB, F-33600 Pessac, France, [§]Department of Chemistry and Biochemistry, Swarthmore College, 500 College Avenue, Swarthmore, Pennsylvania 19081, United States, [⊥]Maintenance des Génomes, Microscopies Moléculaires et Bionanosciences, UMR 8126 CNRS and University of Paris Sud, F-94805 Villejuif, France, [∥]Department of Chemistry, Graduate School of Science, Kyoto University, Kyoto, Japan, and [#]CBMN, CNRS, University of Bordeaux, France. [△]Present address: Department of Molecular Biology, Princeton University, Princeton, NJ 08544-1014, USA.

ABSTRACT

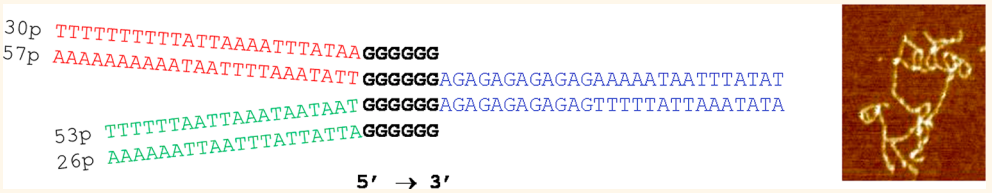

Nucleic acids are finding applications in nanotechnology as nanomaterials, mechanical devices, templates, and biosensors. G-quadruplex DNA, formed by $\pi-\pi$ stacking of guanine (G) quartets, is an attractive alternative to regular B-DNA because of the kinetic and thermodynamic stability of quadruplexes. However, they suffer from a fatal flaw: the rules of recognition, *i.e.*, the formation of a G-quartet in which four *identical* bases are paired, prevent the controlled assembly between different strands, leading to complex mixtures. In this report, we present the solution to this recognition problem. The proposed design combines two DNA elements: parallel-stranded duplexes and a quadruplex core. Parallel-stranded duplexes direct controlled assembly of the quadruplex core, and their strands present convenient points of attachments for potential modifiers. The exceptional stability of the quadruplex core provides integrity to the entire structure, which could be used as a building block for nucleic acid-based nanomaterials. As a proof of principle for the design's versatility, we assembled quadruplex-based 1D structures and visualized them using atomic force and transmission electron microscopy. Our findings pave the way to broader utilization of G-quadruplex DNA in structural DNA nanomaterials.

KEYWORDS: parallel G-quadruplex · guided assembly · nucleic acids · nanotechnology · parallel-stranded duplex · higher order structures

DNA has been used in the design of nanomaterials due to the ability of complementary strands to hybridize in a controllable fashion. In addition, chemical synthesis of DNA is straightforward. A variety of materials based on the strand crossover principle introduced by Seeman[1] and DNA origami introduced by Rothemund[2] have been prepared and characterized. Structures based solely on Watson–Crick base pairing suffer from intrinsic limitations, however, such as low resistance to heating and denaturing reagents, susceptibility to DNases, and flexibility and deformability. In addition, the ability of duplex DNA to conduct electricity is still under debate, and the sensitivity to chemical stimuli is insufficient. As an alternative to duplex DNA, other DNA secondary structures such as G-quadruplexes (G4), triplexes, and DNA junctions should be considered as potential building blocks for nanomaterials.

G-quadruplexes are formed by stacks of four guanines held together by Hoogsteen hydrogen bonding (Figure 1) and have an ion core in the center (that can host a variety of cations, such as Na^+ or K^+) and a negatively charged phosphate backbone. They demonstrate a potentially high conductance,[3] making them appropriate for applications in electronic nanodevices. Parallel G4s with at least four guanine tetrads are exceptionally stable: they resist thermal heating (even boiling) and denaturing conditions (*e.g.*, 7 M urea, 50% formamide). Unlike duplex DNA, G4 structures are stable in up to 50–70% ethanol and are even stabilized by ethanol,[4] methanol, and other dehydrating agents.

* Address correspondence to lyatsun1@swarthmore.edu, jean-louis.mergny@inserm.fr.

Received for review October 24, 2012 and accepted June 13, 2013.

Published online June 13, 2013
10.1021/nn402321g

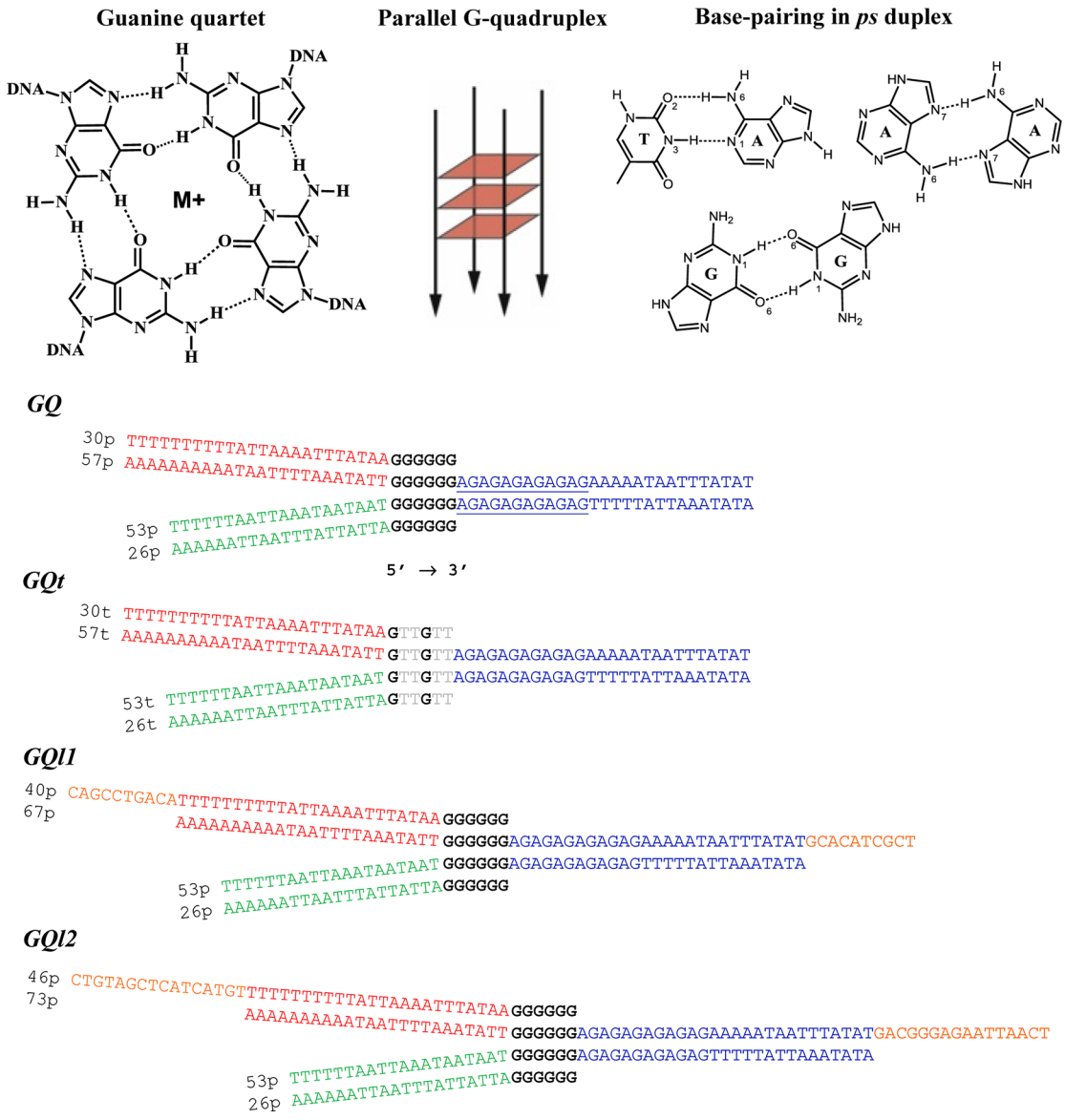

Figure 1. Design and structures of DNA assemblies. All sequences are shown in the 5′ to 3′ direction. *GQ*, *GQl1*, and *GQl2* all contain a quadruplex core highlighted in bold. The regions of parallel-stranded (*ps*) duplex are shown in red, green, and blue. Overhangs complementary to a double-stranded linker are shown in orange.

Tetramolecular G4 structures are stable in the gas phase, as demonstrated by ESI-MS and molecular modeling, and are more robust when imaged by atomic force microscopy.[5] In addition, chemical modification of quadruplexes is straightforward.[6,7] Finally, unlike duplex DNA, G4 assemblies are structurally diverse. Controlled conformational changes of G4 structures can be used in the design of biosensors and molecular devices.[8]

The applications of G4 in nanotechnology are hindered by the quadruplex recognition problem: G-quartets are formed from four identical bases, and, therefore, assembly among strands cannot be controlled. Specifically, a guanine from one G-rich strand can associate with another strand at any of the guanines, or strands can self-associate. In the case of bi- or tetramolecular G4 structures or when more than four G-rich stretches are present in a single oligonucleotide, complex mixtures are obtained instead of well-defined objects. For example, when assembly of tetra-stranded G4 was attempted from two different G-rich strands, 16 (2^4) possible combinations of these strands resulted in five unique G4 structures.[9] In principle, assembly of parallel G4 out of four different strands should result in 256 (4^4) possible strand combinations, leading to 35 unique G4 complexes (Table S1). The quadruplex recognition problem explains why literature reports on G4-based DNA materials with potential nanotechnology applications are relatively sparse.

The first examples of G4-based superstructures came from Sen's lab; this group demonstrated a head-to-tail association of tetra-stranded dT_nG_3 units formed due to a slipped arrangement of the individual

oligonucleotides.[10] Following this work Sen's lab reported G4-mediated synapsable DNA duplex structures.[11] Similarly, Protozanova *et al.* demonstrated the formation of so-called "frayed wires" by $dA_{15}G_{15}$.[12] Another type of G-wire was constructed by the Hendersen lab from the oligomer $dG_4T_2G_4$, making use of its ability to misalign.[5,13] The major drawback of some of these designs is the lack of control over the assembly process. Note that while the term G-wire is used widely in the literature, the conductivity of these structures has not been shown. Recently Kotlyar's laboratory reported efficient preparation of guanine-only nanowires from poly(dG).[14] These wires are long, stiff, heat resistant, mechanically stable, and insensitive to DNase I treatment.[15] However, they do not offer the easy points of attachment necessary for chemical versatility and have little structural diversity. Sugimoto's group designed DNA assemblies based on two components: antiparallel G4 DNA and a canonical Watson–Crick duplex.[16] Our group has recently reported on the assembly of trimolecular quadruplexes using Watson–Crick handles.[17] Overall, more diversity of G4-based nanomaterials and better design are highly desirable.

In this paper, we present a design that overcomes the quadruplex recognition problem. The key to our design is utilization of parallel-stranded (*ps*) duplexes whose role is to direct the formation of the parallel G4 core in a controlled manner. The existence of *ps* DNA secondary structure was first reported in the late 1980s by Jovin's group.[18,19] In principle, *ps* duplex formation is possible for any base pair combination; in reality the existence of competing reactions with Watson–Crick duplex formation places limitations on the sequences and compositions that form *ps* DNA. The secondary structure of a *ps* duplex in our design is maintained by reverse Watson–Crick base pairing between thymine (T) and adenine (A)[18] or alternating, symmetrical self-pairs of $G_{syn}\cdot G_{syn}$ and $A_{anti}\cdot A_{anti}$ in the case of the GA repeat duplex (Figure 1).[20] The reverse Watson–Crick A·T base pair has nearly the same stability as the conventional A·T pair. However, the reverse Watson–Crick G·C base pair has at least one hydrogen bond less than a canonical G·C pair, hence, diminished stability; it was avoided in our design. Overall, optical and biochemical properties of *ps* duplexes differ from those of antiparallel B-DNA. Interestingly, however, *ps* duplexes are reasonably stable under near-physiological conditions, particularly in the presence of Mg^{2+} ions, and have melting temperatures only 10–15 °C lower as compared to their antiparallel counterparts.[19]

Here we report for the first time the design that overcomes the quadruplex recognition problem and leads to rapid and controlled assembly of a parallel-stranded quadruplex DNA structure (referred to as *GQ*) from four different strands facilitated by *ps* duplex formation. The overall architecture and kinetics of *GQ* formation were assessed using gel electrophoresis. The presence of the quadruplex core was demonstrated using CD spectroscopy as well as *via* UV–vis and fluorescent titrations with quadruplex-specific ligands. Thermal properties of the target structure and its duplex components were thoroughly analyzed. As a proof of principle, the *GQ* structure was incorporated into a one-dimensional nanomaterial assembled *via* a variety of linkers based on conventional Watson–Crick hydrogen bonding. The resulting nanomaterial was visualized *via* atomic force microscopy (AFM) and transmission electron microscopy (TEM). This work extends our understanding of controlled assembly of tetrastranded quadruplex-based structures, demonstrates an efficient route to parallel G4 formation, and presents a step toward designing DNA nanomaterials with improved stability and physical properties.

RESULTS AND DISCUSSION

The *GQ* structure was designed based on two distinct elements: (i) the parallel-stranded quadruplex core of six G-quartets and (ii) three *ps* duplexes that guide formation of this quadruplex core. A *parallel* tetra-stranded quadruplex was chosen over bi- or monomolecular quadruplexes because the former is characterized by limited polymorphism, exceptional rigidity, significantly higher thermodynamic stability, and extraordinarily long lifetimes (kinetic inertness) for the same number of G-quartets in both sodium and potassium buffers.[21−24] The sequences of oligonucleotides and assembly patterns are shown in Figure 1. Our design successfully yielded single species out of four different DNA strands in 10 mM lithium cacodylate buffer pH 7.2 and 20 mM $MgCl_2$ (20Mg buffer), as shown by native and denaturing PAGE gels (Figure 2a and Figure S1). The control sequence *GQt*, in which the GGGGGG segment was replaced with GTTGTT to prevent quadruplex formation, was included in all studies. On denaturing gels, the *GQ* structure remained mostly intact, whereas *GQt* dissociated completely into its single-stranded components (Figure 2a). The observed stability of the *GQ* structure is highly desired for possible construction of quadruplex-based DNA nanomaterial.

The *GQ* structure assembly is rapid, requiring less than 10 min for complete folding according to our preliminary kinetics data (not shown). This is truly remarkable, as formation of tetra-stranded DNA structures at comparable concentration (10 μM) is much slower and requires at least an overnight incubation for 70–90% assembly.[23,25] The association of sequences with shorter runs of guanines such as TGGGT is even slower, requiring >24 h even at 100 μM strand concentration.[26] Therefore, *ps* duplexes not only direct the formation of desired GQ structure but also lead to significant acceleration of the assembly process.

To demonstrate unequivocally that the tetra-stranded *GQ* structure contained four different oligonucleotide strands, two sets of experiments were performed: a fluorescent labeling study and a so-called

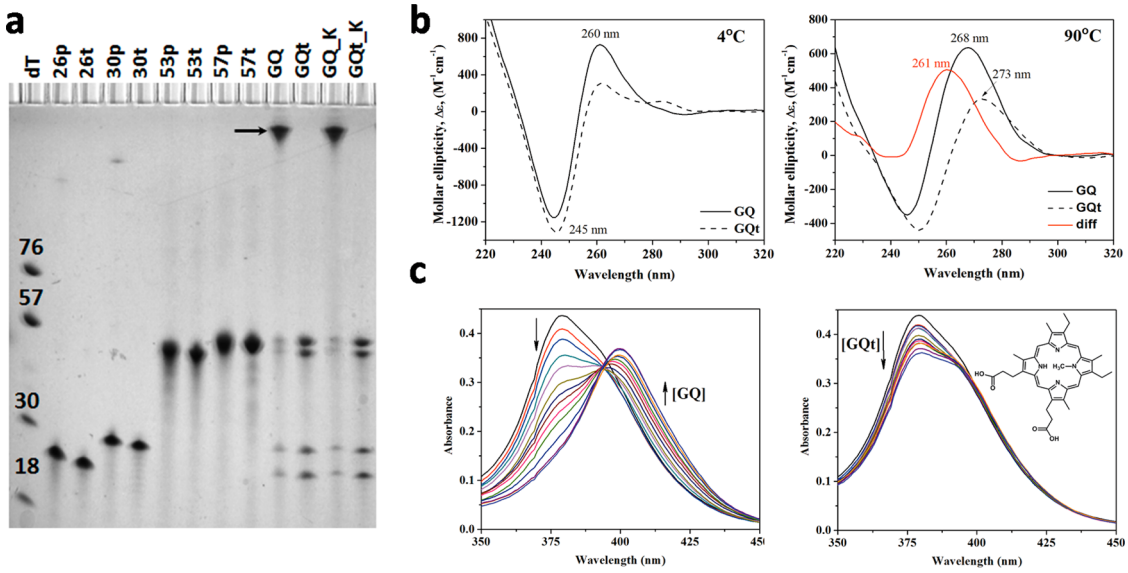

Figure 2. Characterization of *GQ* and *GQt* structures. (a) 10% denaturing PAGE gel containing single-stranded oligonucleotides and *GQ* and *GQt* structures. Lanes marked with K contain samples of *GQ* or *GQt* mixed with 100 mM KCl for 5 min at room temperature before being loaded on the gel. Internal migration markers, dT_{18}, dT_{30}, dT_{57}, and tRNA (76 nt), are provided. Gel was visualized using UV-shadowing. Position of *GQ* is marked with an arrow. (b) CD spectra of *GQ* (peaks at 261 and 245 nm at 4 °C and at 268 and 245 nm at 90 °C) and *GQt* (peaks at 261, 283, and 245 nm at 4 °C and at 273 and 250 nm at 90 °C) in 20Mg buffer. CD difference spectrum (shown in red) was constructed by subtracting the CD signal at 90 °C of *GQt* from that of *GQ*. (c) Representative UV−vis absorption spectra of 3.0 μM NMM titrated with 15 μM *GQ* or *GQt*. The final [*GQ*]/[NMM] was 1.6. Inset shows the structure of NMM.

"missing strand" experiment. In the former case, single-stranded oligonucleotides were labeled with 6-FAM at the 5′ end or with TAMRA at the 3′ end. The presence of fluorescent probes did not alter the migration of single-stranded oligonucleotides to a significant degree, as assessed by PAGE (Figure S2a). These labeled oligonucleotides were used to assemble the following structures: *GQa* (F26p + 30p + 53p + 57p); *GQb* (26p + F30p + 53p + 57p); *GQc* (26p + 30p + 53pT + 57p); and *GQd* (26p + 30p + 53p + 57pT). Each structure contained only one labeled oligonucleotide. The samples were run on a native PAGE gel and visualized using UV shadowing (for total DNA content) and by excitation of the fluorescent probes to determine the incorporation of fluorescently labeled oligonucleotides into the final structure (Figure S2b). The fluorescent probes did not interfere with the mobility of *GQ* assemblies. The gel results indicate that each assembly contained a fluorescently labeled oligonucleotide, supporting the idea that *GQ* is formed indeed out of four different G-rich DNA strands.

Additional support for this conclusion comes from the "missing strand" experiment. In this experiment, *m26, m30, m53*, and *m57* structures ("*m*" stands for missing) were assembled and visualized on native and denaturing gels, Figure S3. In each case only three strands were annealed; for example, 30p, 53p, and 57p (but not 26p) were used to prepare *m26*. None of the *m26, m30, m53*, and *m57* assemblies form species that migrated at the same position as *GQ*, thus demonstrating that all four strands are required to form properly the structure of *GQ*.

The presence of the quadruplex core in the *GQ* structure was verified through circular dichroism (CD), titrations with quadruplex-specific ligands, and dimethyl sulfate (DMS) footprinting experiments. The CD spectra for *GQ* and *GQt* taken at 4 °C are shown in Figure 2b. The CD signals at 245 nm were similar for both assemblies and originated from the *ps* duplex components. The CD spectrum of *GQt* is very similar to the CD reported by Jovin's group for *ps* duplexes only.[19] At 90 °C the CD spectrum for *GQ* indicates the presence of parallel quadruplex structure in agreement with denaturing gel electrophoresis results (Figure 2a), whereas the spectrum for *GQt* is typical of a single-stranded DNA. The *GQ* minus *GQt* difference spectrum at 90 °C contains a single positive peak at 261 nm, typical of a parallel quadruplex structure. The fact that the quadruplex core is intact at 90 °C confirms the remarkable stability of the *GQ* assembly.

The quadruplex-specific ligand *N*-methyl mesoporphyrin IX (NMM) was titrated with *GQ* and with *GQt* and analyzed by UV−vis spectroscopy (Figure 2c). The Soret band of NMM was shifted by 20 nm in the presence of *GQ* and remained unchanged in the presence of *GQt*. A red shift of 17−20 nm has been previously observed upon titration of NMM with a variety of quadruplex structures,[27] but not with calf thymus DNA.[28] This result indicates that a quadruplex core capable of binding NMM was present in *GQ* but not in *GQt*. Recently we showed that NMM is capable of discriminating between parallel and antiparallel quadruplex topologies. Specifically, a red shift of 19.4 nm was observed when NMM was titrated with human telomeric

DNA in potassium buffer (where it forms a parallel or hybrid fold) but not in sodium buffer (where it forms an antiparallel structure).[27] Therefore, the 20 nm red shift of the Soret band observed upon titration of NMM with *GQ* not only proves that the *GQ* structure contains a quadruplex core but also suggests that the quadruplex core has parallel topology.

Ligand 9944 is an ethidium derivative with excellent selectivity toward quadruplex over duplex DNA, as demonstrated in equilibrium dialysis experiments.[29] A substantial increase of fluorescence at 600 nm was observed upon titration of 9944 with *GQ*; a significantly smaller increase of fluorescence was seen upon 9944 titration with *GQt* (Figure S4a and S4b). To determine what caused the increase in fluorescence in the latter case, 9944 was also titrated with a 1:1:1 mixture of *PS1c*, *PS2c*, and *PS3c* (Figure S4c). This mixture represents the sum of all *ps* duplex components of *GQ* (one can think of this mixture as the *GQ* structure minus the quadruplex core). We observed identical increases in fluorescence intensity for 9944 upon titration with this mixture and with *GQt*, indicating that 9944 does interact with *ps* duplexes to some extent. This is the first report of an interaction of 9944 with *ps* duplexes. It is important to note that the interaction of 9944 with *ps* DNA leads to a significantly smaller increase in fluorescence intensity as compared to its interaction with the quadruplex core, especially when one takes into account that the *GQ* assembly has 71 base pairs in its *ps* region and only four to five G-tetrads in its quadruplex core (see below).

Although *GQ* was designed to contain six G-quartets, this number could be lower due to steric strain at the quadruplex/*ps* duplex junction. In order to establish unequivocally how many and which guanines participate in quadruplex formation, we used chemical probing with DMS. Formation of a quadruplex structure protects the N7 of guanines, rendering them resistant to DMS treatment. On the other hand, guanines involved in canonical duplex or *ps* structures are expected to be methylated. These modified bases can be subsequently detected at nucleotide resolution on a sequencing gel after the cleavage of the ^{32}P-labeled oligonucleotide backbone with piperidine (Figure S5). In pure water, single-stranded oligonucleotide 57p was completely degraded by DMS. In 20Mg buffer or this buffer with 50 mM KCl, however, some salt-dependent structure was formed, but all guanines were reactive to a similar extent. When 57p was incorporated within the *GQ* structure, four guanines, G25−G28, were resistant to methylation by DMS in 20Mg buffer, suggesting formation of a four-tetrad quadruplex core. All guanines in a region outside the core, as well as G29 and G30, were methylated by DMS and subsequently cleaved. In 20Mg buffer supplemented with 50 mM KCl, G29 was also protected in addition to G25−G28, suggesting formation of a five-tetrad quadruplex core. In the *GQt* structure, where the GGGGGG segment was replaced with GTTGTT, the remaining two guanines, G25 and G28, were strongly modified by DMS, demonstrating that no guanine tetrads were formed. Overall, DMS footprinting experiments suggest that in physiologically relevant buffer the *GQ* assembly possesses a stable quadruplex core composed of four or five G-tetrads. Importantly, the lifetime of the parallel-stranded quadruplex with five G-tetrad was determined to be $\geq$1 year,[23] signifying kinetic inertness of GQ toward dissociation and its possible utility as a nanomaterial.

The clear advantage of G4-based nanomaterials as compared to those made of duplex DNA is their higher thermal and chemical stability. As described above, *GQ* was stable under denaturing conditions of the gel (boiling in buffer or formamide; presence of urea) or at high temperature, Figure 2a and b. The thermal melting of *GQ* was assessed by CD and UV−vis and was biphasic; the T_m's were 48.0 $\pm$ 1.1 and 59.1 $\pm$ 0.8 °C. In contrast, the melting of *GQt* was monophasic, with a T_m of 44.2 $\pm$ 0.6 °C (Table S3). In both cases, the observed T_m's reflect melting of the *ps* duplexes, as was confirmed by the thermal difference spectra, TDS (Figure S6a). The TDS of *GQ* and *GQt* were almost identical and consistent with the earlier reported TDS signature for *ps* duplexes.[30] The presence of the quadruplex core in *GQ* stabilizes *ps* duplexes by 16.6, 20.0, and 12.8 °C for *PS1c* (red), *PS2c* (green), and *PS3c* (blue), respectively (for details see the Supporting Information (SI)).

We next sought to show that *GQ* can serve as a building block for a variety of higher order structures. In the original design of *GQ* (Figure 1), each end of the three *ps* duplexes may serve as an attachment point for a chemical or protein moiety or for DNA extension. As a proof of principle, we built a one-dimensional (1D) DNA assembly by combining *GQ* with a linker using classical Watson−Crick base pairing (Figure 3a). Note, if the higher order structure is ligated after its assembly, it will retain thermal stability of the quadruplexes. Specifically, at high temperature the *GQ* core will remain intact (as was shown in Figure 2a), holding duplex oligonucleotide components in close proximity to each other. Upon cooling, the entire assembly can return to its original form.

Oligonucleotides 30p and 57p were extended 5′ and 3′, respectively, by either 10 (new oligonucleotides are 40p and 67p) or 16 nucleotides (46p and 73p), and these strands were assembled into *GQl1* and *GQl2* (where *"l"* stands for long). *GQl1* has a region complementary to a 20-nt linker-1, and *GQl2* has a region complementary to a 32-nt linker-2. For ease of detection, we also designed a significantly longer linker, linker-*dx*, to form a 60-base-pair duplex and connect to *GQl2* through a 16-nt complementary overhangs (see Linker Sequences in the SI).

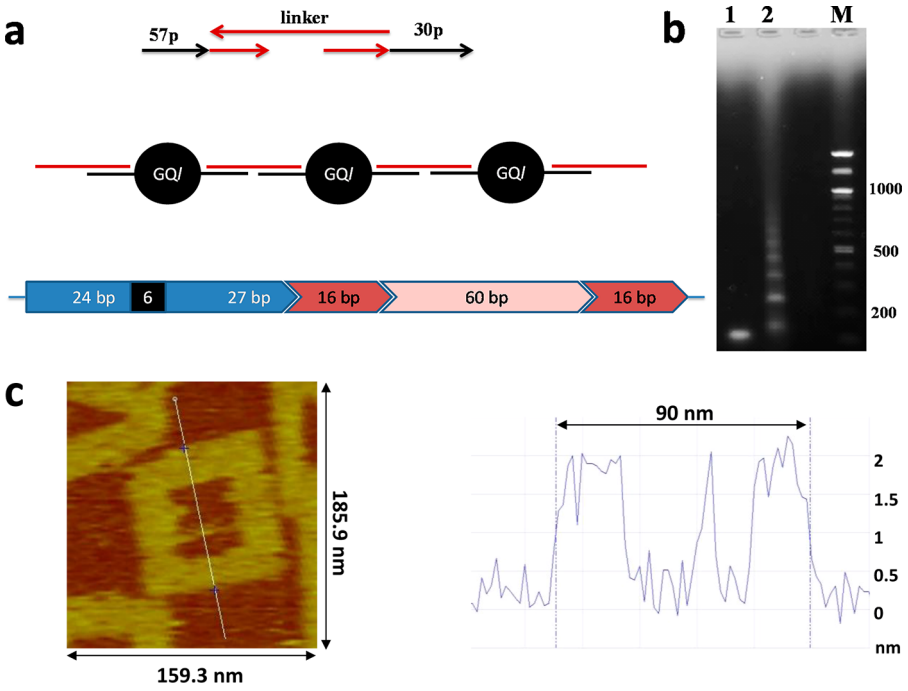

Figure 3. Design and characterization of 1D *GQ*-based DNA assembly. (a) Principles of the design. (Top) Oligonucleotides 30p and 57p were extended 5′ and 3′, respectively, and assembled into *GQl* structures. These structures were combined with a linker through Watson–Crick hydrogen bonding. (Middle) Schematic representation of 1D assembly. (Bottom) Repeating unit of the assembly between *GQl2* and linker-*dx*, which contains, in addition to complementary overhangs, a 60 bp duplex region. *GQl2* is shown in blue (with a quadruplex core in black), linker overlap region is shown in burgundy, and duplex region of the linker is shown in pink. (b) Characterization of 1D structures using 1.3% agarose gel: (lane 1) *GQl1* and (lane 2) *GQl1*+linker-1. (c) *GQl2* structure inserted into DNA origami frame. (Left) Representative AFM image. (Right) Cross section of the DNA origami taken along the line indicated on the AFM image. *GQl2* structures have on average the same height as the origami frame.

All single-stranded oligonucleotides, linkers, and *GQls* were characterized by gel electrophoresis (Figure S7 and data not shown) and displayed the expected mobility. *GQl1* had two melting transitions with T_m's of 48.0 ± 0.5 and 60.4 ± 0.3 °C, similar to the two melting temperatures for *GQ* (Table S3). The TDS signatures of *GQ* and *GQl1* were almost identical (Figure S6a), with a slight increase in absorbance below 240 nm for the latter. These data indicate that addition of overhangs did not alter the overall structure and stability of *GQ*.

Linker-*dx* formed a stable duplex structure that melted at 86.7 °C (Table S3). Its TDS was characterized by a broad peak at 268 nm, and its CD spectra showed a positive peak at 278 nm and a negative peak at 245 nm. These spectroscopic data are consistent with the formation of a 60-bp duplex structure with >50% GC content.[30] On native PAGE, linker-*dx* ran as a single, well-defined band (Figure S7b).

We then determined the stability of the 20-bp duplex designed to hold together *GQ* building blocks in 1D assembly (Figure S8). Details of these experiments are described in the SI. First, the formation of the duplex linker was confirmed using gel electrophoresis. Then the melting temperature of the 20-bp linker itself was measured to be 52.2 ± 0.5 °C. Attachment of *ps* duplexes (marked red and blue in Figure 1) lowered the thermal stability of this linker to 46.8 ± 0.2 °C. We assumed that links between the *GQl2* building block and either linker-2 or linker-*dx* should have even higher thermal stability due to longer regions of overlapping sequence (32 bp *versus* 20 bp).

1D *GQ*-based nanomaterial was prepared by combining preassembled *GQl1* with linker-1 or *GQl2* with linker-2 or linker-*dx* in 20Mg buffer alone or supplemented with 50 mM KCl, 50 mM NaCl, or 1 μM spermidine. Alternatively the nanowires were prepared in a single step by mixing all the components in stoichiometric amounts. These two methods of assembly yielded similar results based on agarose gel analyses (Figure S9a). On agarose gels each building block (*GQl1* and *GQl2*) migrated as a single band of expected size. The higher order structures (*GQl1* + linker-1, *GQl2* + linker-2, *GQl2* + linker-*dx*, *etc.*) migrated either as discrete bands corresponding to up to seven monomers (on a > 1.3% agarose gel, Figure 3b) or as a smear of bands (on a < 1% agarose gel, Figure S9a and S9c), depending on the percent of agarose in the gel and the sizes of the structure. The TDS signature of the higher order structures formed by *GQl1* + linker-1 differed only slightly from the TDS signature of the building block, *GQl1* (Figure S6a). This was expected, as the TDS signatures of *ps* and of Watson–Crick duplexes are rather similar,[30] and melting of the higher order structures leads to dissociation of duplexes but not the quadruplex core.

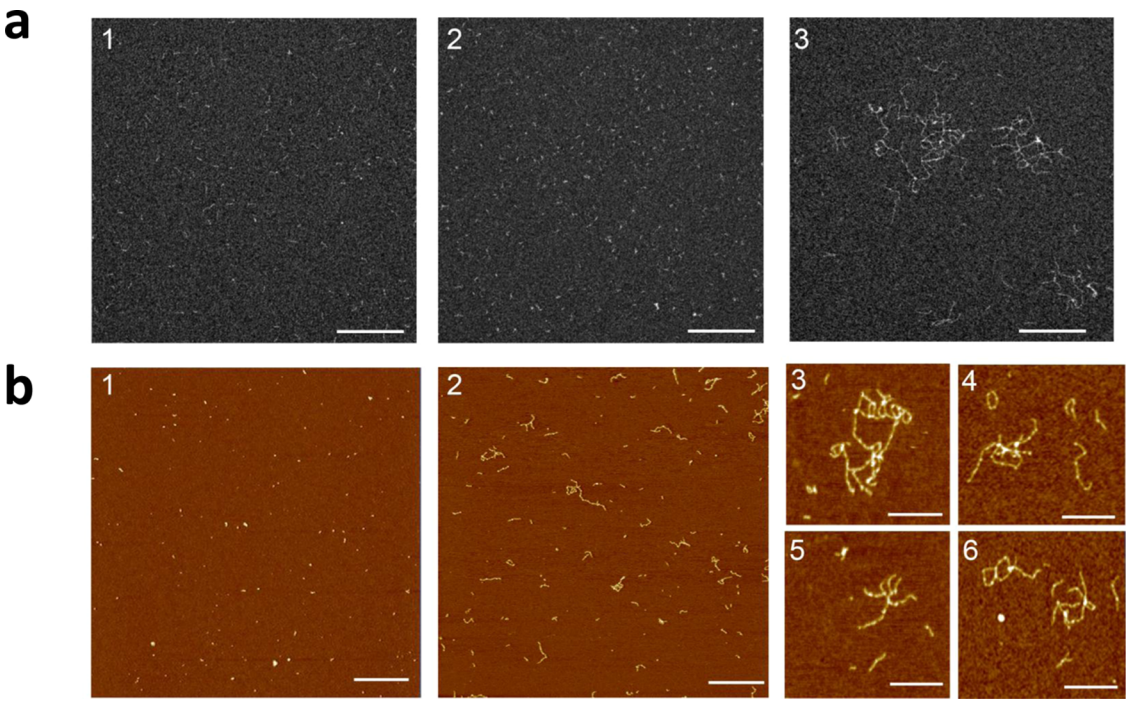

Figure 4. Visualization of GQ-based 1D nanostructures. (a) Representative TEM images of (1) linker-*dx*, measured average length 29 nm, (2) *GQl2*, measured average length 21 nm, and (3) *GQl2*+linker-*dx* at a magnification of 17 600. Scale bars represent 200 nm. (b) Representative AFM images of (1) *GQl2* and (2−6) *GQl2* + linker-*dx*. Scale bars represent 500 nm for panels 1 and 2 and 200 nm for panels 3−6.

We used both AFM and TEM to observe higher order quadruplex-based nanostructures, as each technique has its advantages and drawbacks. TEM provides only two-dimensional imaging; there is no information on height. AFM, while imaging in three-dimensions, has lower lateral resolution as compared to TEM, and the cantilever in AFM may cause collapse of the imaged structures. We began AFM studies by first visualizing the building block, *GQl2*. For ease of detection, this structure was inserted into the DNA origami frame from Sugiyama's lab[31] *via* 16-nt overhangs designed to be complementary to the protrusions in origami, Figure 3c. The height of the *GQl2* structure was approximately 2 nm, comparable to that of the duplex DNA background of the origami. This DNA origami framework was successfully utilized previously to study the dynamics of intermolecular quadruplex formation[32] and DNA methylation by methyltransferase using single-molecule detection by AFM.[31]

The representative TEM and AFM images for *GQ*, linkers, and 1D nanostructures are shown in Figure 4. Statistical analysis of size distribution for these structures is shown in Figure S10. Monomers (*GQl1* and *GQl2*) and linkers (linker-*dx*) appear as small structures of expected size (21 nm for *GQl2* and 29 nm for linker-*dx*) with narrow distribution. Higher order nanostructures appear as wires or bundles of wires of varying length with wide size distribution. The median size is 113 nm, corresponding to two linked monomers, while the longest assemblies contain up to seven monomeric units, in agreement with discrete bands observed on agarose gels (Figure 3b). The height of linker-*dx* and *GQl2* was 1.4−1.6 nm, as expected for a predominantly duplex DNA structure. However, the height of the 1D nanostructures was 0.95−1.1 nm. From X-ray analysis, G-wires and quadruplex structures are expected to be more than 2 nm in diameter. However, the average apparent height of Kotlyar's G-wire that consists exclusively of guanines is only ∼1.6 nm.[15] Like G4-DNA, B-DNA in AFM appears much thinner (0.5−1.1 nm) than its predicted height of 2.0 nm.[33] This discrepancy is also observed in the origami frames.[31] It is conceivable that lower than expected heights result from sample compression or from deformation by the surface forces or by the tip pressure applied to the molecules during AFM imaging.[5] The AFM images of 1D assemblies shown in Figure 4b indicate nonuniform height, most probably due to higher regions of quadruplex cores and lower regions of parallel and antiparallel duplexes.

Although all 1D assemblies produced the expected linear structures, the *GQl2* + linker-*dx* assembly was most readily visualized, probably due to the presence of the long 60-nt duplex in the linker. When 1D assemblies were prepared in the presence of Na^+, Mg^{2+}, or K^+, longer and more aggregated structures were seen in the TEM, in agreement with agarose gels displaying substantially higher molecular weight species (Figure S9b and 9c). Heights of the structures were cation independent. These species might represent

longer or branched assemblies; TEM is consistent with the latter possibility. Branching of the structures can be due to a partial imperfect overlap of Watson–Crick duplex linkers from different *GQ* building blocks.

CONCLUSIONS AND OUTLOOK

This work is the first demonstration of a design in which the guanine–guanine recognition problem is overcome through the use of parallel-stranded duplexes that direct formation of the desired four-stranded quadruplex in a controlled fashion. We showed that the quadruplex assembly process is rapid and structures formed are thermodynamically stable and resistant to denaturing conditions. By designing appropriate overhangs and overlapping linkers we were able to assemble the quadruplex building blocks into 1D nanostructures.

Looking forward, by designing overhangs that contain bimolecular *i*-motifs, assembly could be made pH dependent. We also envision that *GQ* structures could be decorated with biotin or a fluorophore to allow attachment to a surface or to facilitate detection. Finally, incorporation of *GQ* and its 1D polymer into existing DNA nanomaterials will expand the types of available quadruplex-based nanostructures and improve their properties. This work represents another step toward the development of new and exciting DNA-based nanomaterials and nanotechnologies that rely on controlled assembly and have requirements for high thermal and chemical resistance.

METHODS

Materials and Reagents. All oligonucleotides (Table S2) were purchased from Eurogentec and were purified using an RP-Cartridge-Gold. Purities were evaluated using denaturing gel electrophoresis. Prior to use, G-rich oligonucleotides were treated with 50 mM LiOH for 15 min at 37 °C to dissociate undesired quadruplexes. The samples were neutralized with HCl, diluted with 10 mM lithium cacodylate buffer pH 7.2 and 20 mM $MgCl_2$ (20Mg buffer), and used immediately. 20Mg buffer was used in all subsequent experiments. NMM was purchased from Frontier Scientific and handled as described elsewhere.[27] Synthesis and properties of the ethidium derivative 9944 were previously described.[34]

Formation of G4-Based Building Blocks. All quadruplex-based structures and their thermal stabilities are listed in Table S3. The *GQ* structure was formed from an equimolar mixture of oligonucleotides 26p, 30p, 53p, and 57p in 20Mg buffer, annealed at 90 °C for 5 min, cooled on ice for 10 min, and equilibrated at 4 °C overnight before further use. *GQt* was prepared similarly from 26t, 30t, 53t, and 57t oligonucleotides. Structures with fluorescent labels were annealed similarly starting with appropriate oligonucleotides. The *PS1* structure was prepared by annealing 30p with 57p, whereas *PS2* was made from 26p and 53p.

Formation of 1D *GQ*-Based Nanomaterial. The 1D structures were formed from *GQl1* or *GQl2* and an appropriate linker in 20Mg buffer. In some cases buffer was supplemented with 50 mM KCl, 50 mM NaCl, or 1 μM spermidine. Preformed *GQl1* or *GQl2* was mixed with a linker at 1:1 ratio. The linker-*dx* was preformed by annealing 5top and 5bottom oligonucleotides at 90 °C for 5 min followed by cooling on ice for 10 min. The *GQl* + linker mixtures were incubated at 50 °C for 5 min and cooled to 15 °C using a 0.5 °C min^{-1} gradient. We also tested other annealing conditions (see the SI). Alternatively the 1D nanostructures were prepared in a single step by mixing all components at stoichiometric amounts (for example 1:1:1:1:1 of 46p, 73p, 53p, 26p, and linker-1), annealing the mixture at 90 °C for 5 min, cooling on ice for 10 min, followed by overnight equilibration at 4 °C.

Gel Electrophoresis. Native PAGE gels were typically prepared at 6–10% polyacrylamide in 1× Tris-Borate-EDTA (TBE) buffer supplemented with 20 mM $MgCl_2$. Running buffer consisted of 1× TBE with 20 mM $MgCl_2$. Gels were cooled with a water bath and premigrated for 30 min at 3 W. Sucrose was added to all samples (11.5% w/v final) immediately prior to loading gels. Oligothymidylate markers 5′ dT_n (where n = 18, 30, and 57) as well as a 76-nt tRNA were used as internal migration standards. Typically gels were run for 4 h at 3 W; gel temperature did not exceed 16 °C.

Denaturing PAGE gels were typically prepared at 6–20% polyacrylamide containing 1× TBE buffer and 7 M urea; 1× TBE served as running buffer. Samples were boiled for 2 min in 23% v/v formamide before loading gels. Electrophoresis was performed at 14–15 W, and temperatures reached 45–55 °C. The 30 min premigration step was performed for each gel. DNA bands were visualized by UV-shadowing at 254 nm using a fluorescent silica screen (Whatman) on an ETNA-NS ChemiBis 3.2 gel visualization device.

Agarose gels were prepared at 0.6–2% in 1× TBE buffer spiked with ethidium bromide for ease of visualization. Gels were loaded with ~0.3 nmol of DNA (total strands) and run with 0.5–1× TBE supplemented with 2–5 mM $MgCl_2$ at 4 °C, ~90 V, 130 mA for 45–90 min. Ladders of 100 bp and 1 kb (New England BioLabs) were used as migration markers.

DMS Footprinting Experiments. DMS footprinting experiments were carried out following a standard protocol, described in detail in the SI. Briefly, 57p was gel purified, radiolabeled, and treated with DMS (1:400) or with $KMnO_4$ (0.25 mM final) in water, in 20Mg, or in 20Mg with 50 mM KCl. Radiolabeled 57p was used to prepare *GQ*, and this complex was treated with DMS or $KMnO_4$ under identical conditions. DMS footprinting was also performed on the *GQt* structure that was formed using radiolabeled 57t.

Spectroscopic Studies. UV–vis titrations of quadruplex-specific ligand, NMM, with *GQ* and *GQt* were performed on Secomam Uvikon XL or XS spectrophotometers thermostated with an external water bath in 1 cm quartz cuvettes at 20 °C in the 350–670 nm wavelength range. A 400 μL solution of a fixed concentration of porphyrin (3.0–3.5 μM) in 20Mg buffer was titrated by stepwise additions of a ~15 μM stock DNA solution. After each addition of DNA, the resulting mixture was incubated for 4 min and the UV–vis absorbance was recorded. Total volume of DNA added did not exceed 120 μM; the final ratio of [GQ]/[NMM] reached 1.2–1.6. All experiments were run in triplicate. Data were treated as described elsewhere.[35]

Fluorescent titrations of quadruplex-specific ligand, 9944, with *GQ* and *GQt* were performed on a FluoroMax-3 instrument (HORIBA Jobin Yvon) at 20 °C in 0.2 cm quartz cuvettes. The spectra were collected using an excitation wavelength of 450 nm (slit width 5 nm) and an emission wavelength range of 500–800 nm (slit width 5 nm), with 1 scan, 2 nm step size, and 0.5 s averaging time. The overall titration scheme resembles that of NMM UV–vis titrations. All experiments were repeated five times. For additional details on UV–vis titrations of NMM or fluorescent titrations of 9944 see the SI.

For UV–vis melting studies samples were prepared at 0.5 μM and analyzed in 1.0 cm quartz cuvettes. The temperature was measured with the sensor inserted in one of the cuvette holder. Samples were heated from 4 °C to 90 °C and cooled at a rate of 0.15–0.19 °C min^{-1}. Melting data were analyzed assuming a two-state model with temperature-independent enthalpy of unfolding, ΔH.[36] Starting and final baselines (assumed to be linear), melting temperature, T_m, and ΔH were adjusted to get

the best fits. In cases where multiple transitions were observed, the first derivative of the smoothed melting curves was used to estimate T_m. Melting data are summarized in Table S3. Experiments were repeated 4−8 times.

CD wavelength scans were collected in 1 cm quartz cells at 25 °C using a JASCO J-815 spectropolarimeter with a 2 nm bandwidth, 500 nm min^{-1} scan speed, and 1 nm step. Five scans were recorded and averaged. The data were treated as described elsewhere.[35] CD melting was performed on selected structures (*e.g.*, *GQ* and *PS1/PS2*) to confirm UV−vis melting results. The wavelength was monitored at 267, 243, and 335 nm (the latter used as a reference to factor out instrument fluctuations), the averaging time was 8 s, and the bandwidth was 10 nm. Temperature was changed from 4 °C to 90 °C and back at 1 °C min^{-1} rate and a hold time of 5 min at 90 °C. Data at 243 nm were used to determine T_m as described above for UV−vis melting. All data manipulations were done in Origin 8.1.

AFM and TEM. For visualization of *GQl2* structures, we used the DNA frame designed by Sugiyama.[31] This DNA origami was prepared from a circular single-stranded M13mp18 virus genome DNA and 222 short computer-designed staple strands. For DNA frame formation ~15 nM M13mp18 was mixed with an excess of staple strands (8:1) in 20 mM Tris-HCl pH 7.5 buffer with 10 mM EDTA and 10 mM $MgCl_2$. The mixture was annealed by cooling from 85 °C to 15 °C with a temperature gradient of 1 °C min^{-1}. An excess of *GQl2* (5:1) was added to this preformed DNA origami frame and annealed again from 50 °C to 15 °C with a temperature gradient of 0.5 °C min^{-1}. The excess of staple strands and *GQl2* was removed using microspin S300 HR columns (GE Healthcare). The insertion of *GQl2* into the DNA frame was visualized by liquid AFM using a freshly cleaved mica surface without any pretreatment.

AFM on DNA assemblies was performed on a freshly cleaved mica surface treated with 50 μM spermidine for 1 min. An excess of spermidine solution was blotted with filter paper, and 3−5 μL of 5 nM DNA sample was deposited on the mica surface, incubated for 1−2 min, and rinsed with 25 μL of 0.2% (w/v) uranyl acetate. The surface was blotted and dried. For AFM and TEM, samples were prepared in 0.5× TBE and 5 mM $MgCl_2$ with or without 5 mM KCl. Imaging was carried out in tapping mode, with a Multimode system (Bruker) operating with a Nanoscope V controller (Bruker) using silicon AC160TS cantilevers (Olympus) with resonance frequencies of ~300 kHz. All images were collected at a scan frequency of 1 Hz and a resolution of 1024 × 1024 pixels. Images were analyzed with Nanoscope V software. A third-order polynomial function was used to remove the background.

For TEM, 5 μL of a 5 nM DNA sample solution was deposited for 1 min on a 600-mesh copper grid covered with a thin carbon film, activated by glow-discharge in the presence of pentylamine. Grids were washed with aqueous 2% (w/v) uranyl acetate, dried with ashless filter paper, and observed in the dark-field mode with tilted illumination, using a Zeiss 912AB transmission electron microscope. Images were captured at magnifications of 50 000×, 85 000×, and 140 000× with a ProScan 1024 HSC digital camera and iTEM acquisition software (Olympus Soft Imaging Solution). DNA molecule lengths were measured with iTEM software, and length distributions were analyzed with Prism software.

Conflict of Interest: The authors declare no competing financial interest.

Acknowledgment. The authors would like to acknowledge all members of the groups for helpful discussions and technical advice. Financial support was provided by INSERM, University of Bordeaux, Conseil Régional d'Aquitaine (through a Chaire d'Accueil to J.L.M.), Fondation pour la Recherche Médicale, and Agence Nationale de la Recherche (ANR Grants QuantADN, F-DNA, and G4toolbox). J.L.M. dedicates this article to the memory of Steve Kordek and Jean-Louis Leroy.

Supporting Information Available: Additional experimental details; figures of LiOH treatment; characterization of *GQ*, *GQt*, *PS1*, and *PS2* using gel electrophoresis; gels of *GQ* structure formed with one fluorescently labeled oligonucleotide; gels for "missing strand'" experiment; representative fluorescent spectra for 9944 titration with *GQ* and *GQt*; DMS footprinting gels; UV−vis TDS spectra; characterization of *GQl1*, *PSl1*, linker-1, and linker-*dx*; testing stability of linker designed to hold *GQ* monomers together in 1D assembly; characterization of nanostructures *via* agarose gels; characterization of *PS1*, *PS2*, *PS1/PS2*, and control structures; distribution of monomer and 1D structure lengths; table of statistical distribution of *GQ* structures formed from 2 or 4 different strands; list of all oligonucleotides; list of all DNA assemblies and their melting temperatures. This material is available free of charge *via* the Internet at http://pubs.acs.org.

REFERENCES AND NOTES

1. Seeman, N. C. Nanomaterials based on DNA. *Annu. Rev. Biochem.* **2010**, *79*, 65–87.
2. Rothemund, P. W. K. Folding DNA to create nanoscale shapes and patterns. *Nature* **2006**, *440*, 297–302.
3. Liu, S.-P.; Weisbrod, S. H.; Tang, Z.; Marx, A.; Scheer, E.; Erbe, A. Direct measurement of electrical transport through G-quadruplex DNA with mechanically controllable break junction electrodes. *Angew. Chem., Int. Ed.* **2010**, *49*, 3313–3316.
4. Vorlíčková, M.; Bednářová, K.; Kypr, J. Ethanol is a better inducer of DNA guanine tetraplexes than potassium cations. *Biopolymers* **2006**, *82*, 253–260.
5. Marsh, T. C.; Vesenka, J.; Henderson, E. A new DNA nanostructure, the G-wire, imaged by scanning probe microscopy. *Nucleic Acids Res.* **1995**, *23*, 696–700.
6. Gros, J.; Rosu, F.; Amrane, S.; De Cian, A.; Gabelica, V.; Lacroix, L.; Mergny, J.-L. Guanines are a quartet's best friend: impact of base substitutions on the kinetics and stability of tetramolecular quadruplexes. *Nucleic Acids Res.* **2007**, *35*, 3064–3075.
7. Saccà, B.; Lacroix, L.; Mergny, J.-L. The effect of chemical modifications on the thermal stability of different G-quadruplex-forming oligonucleotides. *Nucleic Acids Res.* **2005**, *33*, 1182–1192.
8. Alberti, P.; Mergny, J.-L. DNA duplex−quadruplex exchange as the basis for a nanomolecular machine. *Proc. Natl. Acad. Sci. U.S.A.* **2003**, *100*, 1569–1573.
9. Tran, P. L. T.; Moriyama, R.; *et al.* A mirror-image tetramolecular DNA quadruplex. *Chem. Comm.* **2011**, *47* (19), 5437−5439.
10. Sen, D.; Gilbert, W. Novel DNA superstructures formed by telomere-like oligomers. *Biochemistry* **1992**, *31*, 65–70.
11. Fahlman, R. P.; Sen, D. Cation-regulated self-association of "synapsable" DNA duplexes. *J. Mol. Biol.* **1998**, *280*, 237–244.
12. Protozanova, E.; Macgregor, R. B. Frayed wires: a thermally stable form of DNA with two distinct structural domains. *Biochemistry* **1996**, *35*, 16638–16645.
13. Marsh, T. C.; Henderson, E. G-Wires: self-assembly of a telomeric oligonucleotide, d(GGGGTTGGGG), into large superstructures. *Biochemistry* **1994**, *33*, 10718–10724.
14. Borovok, N.; Molotsky, T.; Ghabboun, J.; Porath, D.; Kotlyar, A. Efficient procedure of preparation and properties of long uniform G4-DNA nanowires. *Anal. Biochem.* **2008**, *374*, 71–78.
15. Kotlyar, A. B.; Borovok, N.; Molotsky, T.; Cohen, H.; Shapir, E.; Porath, D. Long, Monomolecular Guanine-Based Nanowires. *Adv. Mater.* **2005**, *17*, 1901–1905.
16. Dutta, K.; Fujimoto, T.; Inoue, M.; Miyoshi, D.; Sugimoto, N. Development of new functional nanostructures consisting of both DNA duplex and quadruplex. *Chem. Commun.* **2010**, *46*, 7772–7774.
17. Zhou, J.; Bourdoncle, A.; Rosu, F.; Gabelica, V.; Mergny, J.-L. Tri-G-quadruplex: controlled assembly of a G-quadruplex structure from three G-rich strands. *Angew. Chem., Int. Ed.* **2012**, *51*, 11002–11005.
18. Van de Sande, J. H.; Ramsing, N. B.; Germann, M. W.; Elhorst, W.; Kalisch, B. W.; von Kitzing, E.; Pon, R. T.; Clegg, R. C.; Jovin, T. M. Parallel stranded DNA. *Science* **1988**, *241*, 551–557.
19. Ramsing, N. B.; Jovin, T. M. Parallel stranded duplex DNA. *Nucleic Acids Res.* **1988**, *16*, 9892.

20. Rippe, K.; Fritsch, V.; Westhof, E.; Jovin, T. M. Alternating d(G-A) sequences form a parallel-stranded DNA homoduplex. *EMBO* **1992**, *11*, 3777–3786.
21. Hardin, C. C.; Henderson, E.; Watson, T.; Prosser, J. K. Monovalent cation induced structural transitions in telomeric DNAs: G-DNA folding intermediates. *Biochemistry* **1991**, *30*, 4460–4472.
22. Lu, M.; Guo, Q.; Kallenbach, N. R. Thermodynamics of G-tetraplex formation by telomeric DNAs. *Biochemistry* **1993**, *32*, 598–601.
23. Bardin, C.; Leroy, J. L. The formation pathway of tetramolecular G-quadruplexes. *Nucleic Acids Res.* **2008**, *36*, 477–488.
24. Šket, P.; Plavec, J. Tetramolecular DNA quadruplexes in solution: insights into structural diversity and cation movement. *J. Am. Chem. Soc.* **2010**, *132*, 12724–12732.
25. Mergny, J.-L.; De Cian, A.; Ghelab, A.; Saccà, B.; Lacroix, L. Kinetics of tetramolecular quadruplexes. *Nucleic Acids Res.* **2005**, *33*, 81–94.
26. De Cian, A.; Mergny, J.-L. Quadruplex ligands may act as molecular chaperones for tetramolecular quadruplex formation. *Nucleic Acids Res.* **2007**, *35*, 2483–2493.
27. Nicoludis, J. M.; Barrett, S. P.; Mergny, J.-L.; Yatsunyk, L. A. Interaction of human telomeric DNA with N-methyl mesoporphyrin IX. *Nucleic Acids Res.* **2012**, *40*, 5432–5447.
28. Arthanari, H.; Basu, S.; Kawano, T. L.; Bolton, P. H. Fluorescent dyes specific for quadruplex DNA. *Nucleic Acids Res.* **1998**, *26*, 3724–3728.
29. Ragazzon, P.; Chaires, J. B. Use of competition dialysis in the discovery of G-quadruplex selective ligands. *Methods* **2007**, *43*, 313–323.
30. Mergny, J.-L.; Li, J.; Lacroix, L.; Amrane, S.; Chaires, J. B. Thermal difference spectra: a specific signature for nucleic acid structures. *Nucleic Acids Res.* **2005**, *33*, e138.
31. Endo, M.; Katsuda, Y.; Hidaka, K.; Sugiyama, H. Regulation of DNA methylation using different tensions of double strands constructed in a defined DNA nanostructure. *J. Am. Chem. Soc.* **2010**, *132*, 1592–1597.
32. Sannohe, Y.; Endo, M.; Katsuda, Y.; Hidaka, K.; Sugiyama, H. Visualization of dynamic conformational switching of the G-quadruplex in a DNA nanostructure. *J. Am. Chem. Soc.* **2010**, *132*, 16311–16313.
33. Kasumov, A. Y.; Klinov, D. V.; Roche, P. E.; Guéron, S.; Bouchiat, H. Thickness and low-temperature conductivity of DNA molecules. *Appl. Phys. Lett.* **2004**, *84*, 1007–1009.
34. Koeppel, F.; Riou, J.-F.; Laoui, A.; Mailliet, P.; Arimondo, P. B.; Labit, D.; Petitgenet, O.; Hélène, C.; Mergny, J.-L. Ethidium derivatives bind to G-quartets, inhibit telomerase and act as fluorescent probes for quadruplexes. *Nucleic Acids Res.* **2001**, *29*, 1087–1096.
35. Bhattacharjee, A. J.; Ahluwalia, K.; Taylor, S.; Jin, O.; Nicoludis, J. M.; Buscaglia, R.; Brad Chaires, J.; Kornfilt, D. J. P.; Marquardt, D. G. S.; Yatsunyk, L. A. Induction of G-quadruplex DNA structure by Zn(II) 5,10,15,20-tetrakis-(N-methyl-4-pyridyl)porphyrin. *Biochimie* **2011**, *93*, 1297–1309.
36. Ramsay, G. D.; Eftink, M. R. Analysis of multidimensional spectroscopic data to monitor unfolding of proteins. *Methods Enzymol.* **1994**, *240*, 615–645.